

# The chronic heart failure evolutions: Different fates and routes

Piergiuseppe Agostoni<sup>1,2\*</sup>, Mattia Chiesa<sup>1,3</sup>, Elisabetta Salvioni<sup>1</sup>, Michele Emdin<sup>4,5</sup>, Massimo Piepoli<sup>6,7</sup>, Gianfranco Sinagra<sup>8</sup>, Michele Senni<sup>9</sup>, Alice Bonomi<sup>1</sup>, Stamatis Adamopoulos<sup>10</sup>, Dimitris Miliopoulos<sup>10</sup>, Massimo Mapelli<sup>1,2</sup>, Jeness Campodonico<sup>1</sup>, Umberto Attanasio<sup>11</sup>, Anna Apostolo<sup>1</sup>, Emanuele Pestrin<sup>12</sup>, Agostino Rossoni<sup>13</sup>, Damiano Magri<sup>14</sup>, Stefania Paolillo<sup>15</sup>, Ugo Corrà<sup>16</sup>, Rosa Raimondo<sup>17</sup>, Antonio Cittadini<sup>18,19</sup>, Annamaria Iorio<sup>9</sup>, Andrea Salzano<sup>20,21</sup>, Rocco Lagioia<sup>22</sup>, Carlo Vignati<sup>1</sup>, Roberto Badagliacca<sup>23</sup>, Pasquale Perrone Filardi<sup>24</sup>, Michele Correale<sup>25</sup>, Enrico Perna<sup>26</sup>, Marco Metra<sup>27</sup>, Gaia Cattadori<sup>28</sup>, Marco Guazzi<sup>29</sup>, Giuseppe Limongelli<sup>30</sup>, Gianfranco Parati<sup>31,32</sup>, Fabiana De Martino<sup>33</sup>, Maria Vittoria Matassini<sup>34</sup>, Francesco Bandera<sup>35,36</sup>, Maurizio Bussotti<sup>37</sup>, Federica Re<sup>38</sup>, Carlo M. Lombardi<sup>27</sup>, Angela B. Scardovi<sup>39</sup>, Susanna Sciomer<sup>23</sup>, Andrea Passantino<sup>40</sup>, Caterina Santolamazza<sup>26</sup>, Davide Girola<sup>41</sup>, Claudio Passino<sup>4</sup>, Marlus Karsten<sup>1,42</sup>, Savina Nodari<sup>43</sup>, Giulio Pompilio<sup>1,44</sup> and on behalf of MECKI score research group<sup>6</sup>

<sup>1</sup>Centro Cardiologico Monzino, IRCCS, Milan, Italy; <sup>2</sup>Department of Clinical Sciences and Community Health, Section of Cardiology, University of Milan, Milan, Italy; <sup>3</sup>Department of Electronics, Information and Biomedical Engineering, Politecnico di Milano, Milan, Italy; <sup>4</sup>Health Science Interdisciplinary Center, Scuola Superiore Sant'Anna, Pisa, Italy; <sup>5</sup>Cardio-Thoracic Department, Fondazione Toscana Gabriele Monasterio, Pisa, Italy; <sup>6</sup>Department of Clinical Cardiology, IRCCS Policlinico San Donato, Milan, Italy; <sup>7</sup>Department of Biomedical Sciences for Health, University of Milan, Milan, Italy; <sup>8</sup>Department of Cardiology, 'Azienda Sanitaria Universitaria Giuliano-Isontina', Trieste, Italy; <sup>9</sup>Department of Cardiology, Unit of Cardiology, ASST Papa Giovanni XXIII, Bergamo, Italy; <sup>10</sup>Heart Failure and Heart Transplant Units, Onassis Cardiac Surgery Centre, Attica, Greece; <sup>11</sup>Federico II University, Naples, Italy; <sup>12</sup>Università degli studi di Trieste, Trieste, Italy; <sup>13</sup>Università degli studi Milano Bicocca, Milan, Italy; <sup>14</sup>Department of Clinical and Molecular Medicine, Azienda Ospedaliera Sant'Andrea, 'Sapienza' Università degli Studi di Roma, Rome, Italy; <sup>15</sup>Dipartimento di scienze biomediche avanzate, Federico II University, Naples, Italy; <sup>16</sup>Department of Cardiology, Istituti Clinici Scientifici Maugeri, IRCCS, Veruno Institute, Veruno, Italy; <sup>17</sup>Divisione di Cardiologia Riabilitativa, Istituti Clinici Scientifici Maugeri, Varese, Italy; <sup>18</sup>Department of Translational Medical Sciences, Federico II University, Naples, Italy; <sup>19</sup>Interdepartmental Center for Gender Medicine Research 'GENESIS', Naples, Italy; <sup>20</sup>Cardiac Unit, AORN A Cardarelli, Naples, Italy; <sup>21</sup>Department of Cardiovascular Sciences, University of Leicester, Leicester, UK; <sup>22</sup>UOC Cardiologia di Riabilitativa, Mater Dei Hospital, Bari, Italy; <sup>23</sup>Dipartimento di Scienze Cliniche, Internistiche, Anestesiologiche e Cardiovascolari, 'Sapienza', Rome University, Rome, Italy; <sup>24</sup>Department of Advanced Biomedical Sciences, Federico II University of Naples and Mediterranean CardioCentro, Naples, Italy; <sup>25</sup>Department of Cardiology, University of Foggia, Foggia, Italy; <sup>26</sup>Dipartimento cardio-toraco-vascolare, Ospedale Cà Granda- A.O. Niguarda, Milan, Italy; <sup>27</sup>Department of Cardiology, Department of Medical and Surgical Specialties, Radiological Sciences, and Public Health, University of Brescia, Brescia, Italy; <sup>28</sup>Unità Operativa Cardiologia Riabilitativa, IRCCS Multimedica, Milan, Italy; <sup>29</sup>University of Milano, Milan, Italy; <sup>30</sup>Cardiologia SUN, Ospedale Monaldi (Azienda dei Colli), Seconda Università di Napoli, Naples, Italy; <sup>31</sup>Department of Cardiovascular, Neural and Metabolic Sciences, San Luca Hospital, Istituto Auxologico Italiano, IRCCS, Milan, Italy; <sup>32</sup>Department of Medicine and Surgery, University of Milano-Bicocca, Milan, Italy; <sup>33</sup>Unità funzionale di cardiologia, Casa di Cura Tortorella, Salerno, Italy; <sup>34</sup>Department of Cardiology, Division of Cardiac Intensive Care Unit-Cardiology, Ospedali Riuniti di Ancona, Ancona, Italy; <sup>35</sup>Department of Biomedical Sciences for Health, University of Milano, Milan, Italy; <sup>36</sup>Department of Cardiology, IRCCS Policlinico San Donato, Milan, Italy; <sup>37</sup>Cardiac Rehabilitation Unit, Istituti Clinici Scientifici Maugeri, IRCCS, Scientific Institute of Milan, Milan, Italy; <sup>38</sup>Division of Cardiology, Cardiac Arrhythmia Center and Cardiomyopathies Unit, San Camillo-Forlanini Hospital, Rome, Italy; <sup>39</sup>Division of Cardiology, Santo Spirito Hospital, Rome, Italy; <sup>40</sup>Division of Cardiology, Istituti Clinici Scientifici Maugeri, Institute of Bari, Bari, Italy; <sup>41</sup>Clinica Hildebrand, Centro di Riabilitazione Brissago, Brissago, Switzerland; <sup>42</sup>Programa de Pós-Graduação em Fisioterapia, UDESC, Florianópolis, Brazil; <sup>43</sup>Department of Medical and Surgical Specialties, Radiological Sciences and Public Health, University of Brescia Medical School, Brescia, Italy; and <sup>44</sup>Department of Biomedical, Surgical and Dental Sciences, Università degli Studi di Milano, Milan, Italy

## Abstract

**Aims** Individual prognostic assessment and disease evolution pathways are undefined in chronic heart failure (HF). The application of unsupervised learning methodologies could help to identify patient phenotypes and the progression in each phenotype as well as to assess adverse event risk.

**Methods and results** From a bulk of 7948 HF patients included in the MECKI registry, we selected patients with a minimum 2-year follow-up. We implemented a topological data analysis (TDA), based on 43 variables derived from clinical, biochemical, cardiac ultrasound, and exercise evaluations, to identify several patients' clusters. Thereafter, we used the trajectory analysis to describe the evolution of HF states, which is able to identify bifurcation points, characterized by different follow-up paths, as well as specific end-stages conditions of the disease. Finally, we conducted a 5-year survival analysis (composite of cardiovascular death, left ventricular assist device, or urgent heart transplant). Findings were validated on internal ( $n = 527$ ) and external ( $n = 777$ ) populations. We analyzed 4876 patients (age = 63 [53–71], male gender  $n = 3973$  (81.5%), NYHA class I–II  $n = 3576$  (73.3%), III–IV  $n = 1300$  (26.7%), LVEF = 33 [25.5–39.9], atrial fibrillation  $n = 791$  (16.2%), peak  $\text{VO}_2\%$  pred = 54.8

[43.8–67.2]), with a minimum 2-year follow-up. Nineteen patient clusters were identified by TDA. Trajectory analysis revealed a path characterized by 3 bifurcation and 4 end-stage points. Clusters survival rate varied from 44% to 100% at 2 years and from 20% to 100% at 5 years, respectively. The event frequency at 5-year follow-up for each study cohort cluster was successfully compared with those in the validation cohorts ( $R = 0.94$  and  $R = 0.84$ ,  $P < 0.001$ , for internal and external cohort, respectively). Finally, we conducted a 5-year survival analysis (composite of cardiovascular death, left ventricular assist device, or urgent heart transplant observed in 22% of cases).

**Conclusions** Each HF phenotype has a specific disease progression and prognosis. These findings allow to individualize HF patient evolutions and to tailor assessment.

**Keywords** Cardiopulmonary exercise test; Heart failure; Prognosis; Topological data analysis

Received: 13 March 2024; Revised: 9 May 2024; Accepted: 24 June 2024

\*Correspondence to: Piergiuseppe Agostoni, Department of Clinical Sciences and Community Health, Section of Cardiology, Centro Cardiologico Monzino, IRCCS, University of Milan, Via Parea, 4, 20138 Milan, Italy. Email [piergiuseppe.agostoni@unimi.it](mailto:piergiuseppe.agostoni@unimi.it); [piergiuseppe.agostoni@ccfm.it](mailto:piergiuseppe.agostoni@ccfm.it)  
Details for the MECKI score research group are provided in Appendix A.

## Introduction

An accurate and individualized prognostic assessment of patients suffering from chronic heart failure (HF) in order to identify those at higher risk of complications and ominous outcome is still an unmet need.<sup>2</sup> A better patients' stratification will allow identification of candidates who need treatment upgrading and tailoring, personalization of follow-up and optimized resource allocation. Currently, clinical definitions classify HF according to left ventricle ejection fraction and HF aetiology<sup>2</sup> while several parameters are used to define HF severity including plasma level of B-type natriuretic peptides, exercise derived data, haemoglobin concentration, iron deficiency or overload, kidney function, presence of HF co-morbidities and, more recently, proteomic derived data to assess inflammation, redox state, and coagulation.<sup>3–7</sup> Regardless, at present, none of the several HF prognostic tools alone or in combination consents to precisely define a reliable HF evolution model.<sup>8–12</sup> Moreover, on top of prognosis, it is important to properly phenotyping HF patients to understand who of the HF patients' plethora will negatively evolve toward a higher risk condition and possibly how fast this evolution will be. With this regard, of major importance is the identification of specific conditions or parameters changes leading to or being a marker of a change in HF evolution trajectory.<sup>1</sup> Indeed, characterizing subgroups of patients at variable risk and HF evolution is crucial to improve the decision-making process in HF.

In this context, the application of unsupervised learning methodologies could help the identification of specific patient phenotypes with predictable HF evolution and possibly with a predictable speed of this evolution. Among them, topological data analysis (TDA) is a robust and effective unsupervised methodology, able to preserve the intrinsic characteristics of data and the mutual relations among observations, depicting complex data in a graph-based representation.<sup>13</sup> Indeed, building topological models as networks, TDA allows complex diseases to be inspected in a con-

tinuous space, where subjects can 'fluctuate' over the graph, sharing, at the same time, more than one adjacent node of the network.<sup>14</sup> Of note, TDA has proved to be able to identify specific 'communities' of patients revealing similar clinical characteristics, for example, those diagnosed with diabetes, coronary artery disease, or aortic stenosis.<sup>15–18</sup>

The purpose of the present work was a multi-step analysis of a sizable population of HF patients studied in a holistic mode including demographic, clinical, therapy, laboratory, cardiac ultrasound, and exercise data with a precise predefined follow-up. At first, we aimed to identify HF patients' phenotypes (communities) who share several characteristics. Second, we wanted to identify the possible evolution pathways of each HF patients' community and, finally, to assess the risk of adverse events in each HF patients' community.

## Methods

The present study considers the MECKI registry population, enrolled between 1993 and 2022 from 26 Italian sites for a bulk of 7948 patients with an average follow-up of 4.09 [1.78–7.47] and unfixed HF severity.<sup>3</sup> In the present analysis, a minimum 2-year follow-up was considered since the original MECKI score refers to a 2-year prognosis. Inclusion criteria for the MECKI study are the following: previous or present HF symptoms (NYHA functional class I–IV) and history or presence of left ventricular ejection fraction (LVEF)  $< 40\%$ , unchanged HF medications for at least 3 months, ability to perform a CPET, and no major cardiovascular treatment or intervention scheduled. Exclusion criteria were history of pulmonary embolism, moderate-to-severe aortic and mitral stenosis, pericardial disease, severe obstructive lung disease, exercise-induced angina and significant electrocardiographic (ECG) alterations, or presence of any clinical co-morbidity interfering with exercise performance. A requirement for inclusion in the registry was a CPET performed with the

following modalities: (1) a ramp exercise on an electronically braked cycle ergometer with a protocol set, to reach peak exercise in 8 to 12 min<sup>19</sup>; (2) symptom limited tests, regardless of the respiratory exchange ratio (RER) reached. Ventilation and respiratory gases were collected breath-by-breath and analyzed following a standard technique.<sup>20</sup> Oxygen uptake at peak exercise (peakVO<sub>2</sub>) was calculated as the 20-s average of the highest recorded VO<sub>2</sub>, while ventilation vs. CO<sub>2</sub> production slope (VE/VCO<sub>2</sub> slope) was calculated as the slope of the linear relationship between VE and VCO<sub>2</sub> from one minute after the beginning of loaded exercise to the end of the isocapnic buffering period. Peak VO<sub>2</sub> expressed as % of predicted value (VO<sub>2</sub>%) was calculated according to Hansen *et al.*<sup>21</sup> In addition to CPET-related variables, the MECKI registry collects echocardiographic, ECG, therapy, and blood chemistry data at enrolment, as well as records vital status and causes of events during follow-up. Patient follow-up and data management procedures were performed as previously described.<sup>3</sup> In brief, follow-up was carried out according to the local HF programme, and it ended with the last clinical evaluation or with patients' death, heart transplantation, and left ventricular assist device (LVAD) implantation. If a patient died after hospital discharge, medical records of the event and the reported cause of death were collected. For prognosis evaluation, the endpoint was the composite of cardiovascular death, urgent heart transplantation, or LVAD implantation. The study was approved by the local ethics committee (protocol number: CCM04\_21 PA).

The present multi-steps study consists in a data pre-processing phase to consolidate the MECKI score dataset, in an unsupervised analysis aimed at identification of the study cohorts by TDA, communities' characterization and trajectory inference and, finally, in a supervised analysis for risk assessment and results validation (*Figure 1*).

## Topological data analysis

TDA needs some parameters to be properly assessed and set.<sup>13</sup> The first 2 dimensions extracted from the principal component analysis (PCA) have been chosen as lenses, while the number of TDA bins (NB) and the bin overlapping ratio (BO) have been selected via a 'grid search' approach, ranging NB between<sup>20–32</sup> and BO between [0.2–0.5]. To ensure a scale-free configuration of the resulted network, the lowest Pearson's R correlation index between node rank (k) and the frequency of node rank (p(k)) has been chose as evaluation metrics. The best parameters' set was: NB = 28 and OB = 0.2 (see details on the Supplementary File). TDA was performed by the 'PIUMA' R package (<https://bioconductor.org/packages/devel/bioc/html/PIUMA.html>). Networks have been built and enriched by Cytoscape,<sup>22</sup> each node represents a group of patients with similar characteristics, while edges thickness depicts the number of samples shared by nodes

(Jaccard Index). Edges with a Jaccard Index > 0.1 were considered; on the other hand, nodes collecting <2 patients or without any connections were used as a validation cohort (see below). The Girvan–Newman algorithm implemented in the 'clustermaker2' Cytoscape plug-in, in which edges are iteratively removed based on the value of their betweenness, was used to identify communities (i.e., clusters) in the network.<sup>23</sup> Of note the cluster labels were randomly assigned.

## Trajectory analysis

Trajectory analysis allows deriving paths, that is, trajectories, that describe the evolution of samples traversing through different states and, at the same time, estimating a temporal unit, called pseudo-time, which describes the progression from a state to the next one; this method was firstly proposed to model single cell RNA-seq experiments.<sup>24</sup> Of note, during their HF journey, patients may progressively increase or reduce their pseudo-time in case of HF worsening or improvement, respectively. Here, we assumed that each cluster is a disease state. Network nodes were projected onto a 2D space by the 'Uniform Manifold Approximation and Projection' (UMAP) dimension reduction method, implemented in the 'umap' (v.0.2.10) R package.<sup>25</sup> Then, the 'slingshot' R package was exploited to identify the clusters' centroids, assess clusters' relationships, determine trajectories and, then, infer pseudo-times. Overall, this analysis allows inferring 'state-by-state', the sequence and the progression of a disease, iteratively assessing the lowest difference between all adjacent clusters' characteristics.<sup>26</sup>

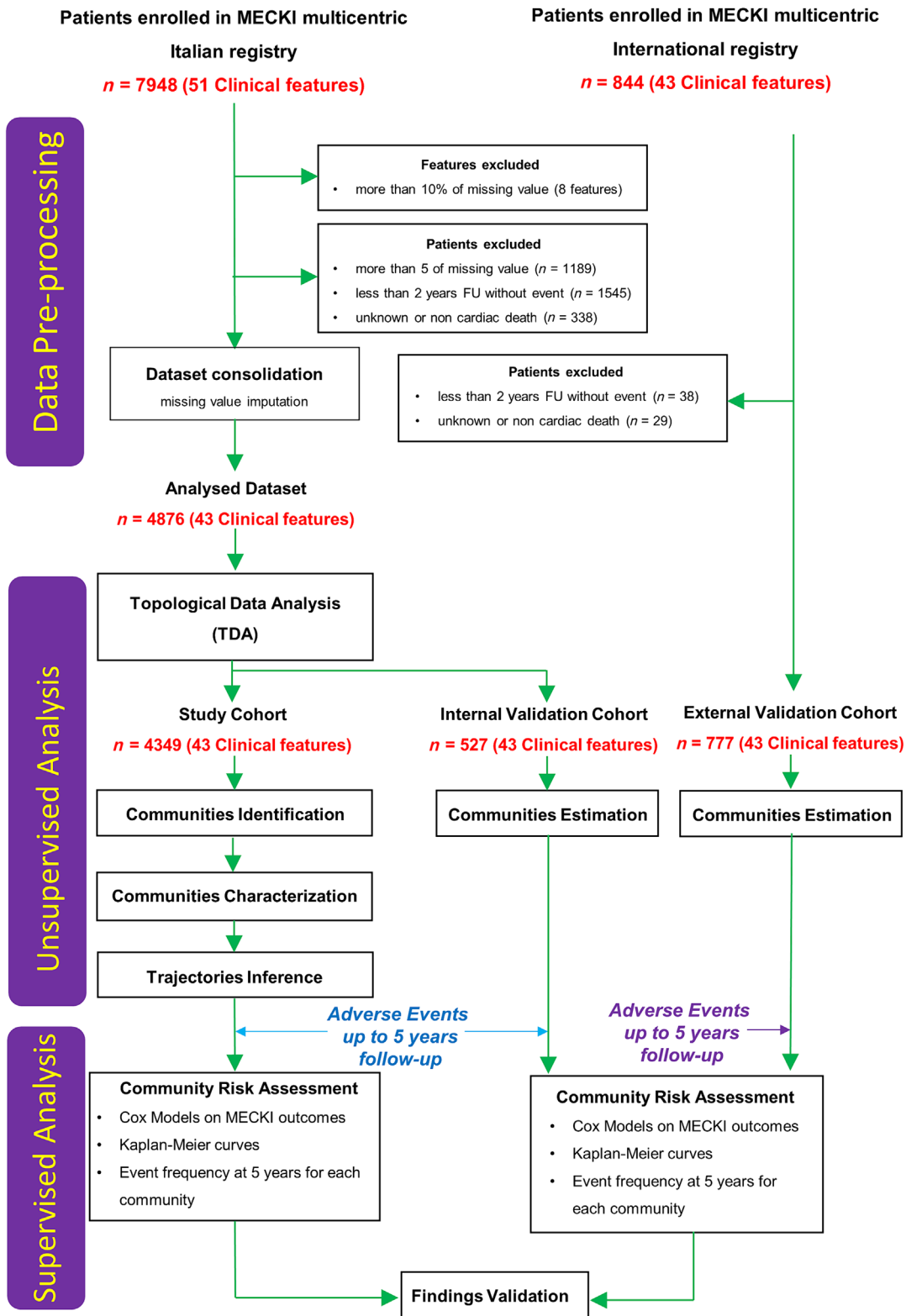
## Survival analysis

Survival analyses were performed, exploiting the 'survival' (v. 3.2.13) and 'survminer' (v. 0.4.9) R packages.<sup>27</sup> Kaplan–Meier analysis was implemented to generate time-to-event curves up to five-year follow-up in patients with and without reaching the study endpoint, recorded in the MECKI registry. All patients included in the study (study cohort and internal + external validation cohorts, *Figure 1*) were considered in the survival analysis. A *P*-value < 0.05 was considered statistically significant.

## Internal and external validation

The cohort for the internal validation was built with patients not resulted to be connected to any nodes of the network generated by TDA (*n* = 527). On the other hand, the cohort for the external validation was gathered by collecting data from European and Chinese centres, joining the MECKI consortium activities on December 2022 (*n* = 777). Data of the latter patients were recently published.<sup>28</sup>

**Figure 1** Study workflow. The block diagram describes the implemented analysis which are categorized in three main steps: data pre-processing, the unsupervised analysis (cluster identification, cluster characterization and trajectories inference), and the supervised analysis (survival analysis and validations).



Downloaded from https://academic.oup.com/ehf/article/12/1/14/188261822 by Fondazione Centro S. Raffaele user on 02 April 2026

For both the validation cohorts, patients were assigned to a specific cluster based on their features' similarity with the clusters' hallmarks, identified by the TDA on the study cohort; specifically, for each cluster, a coefficient of variation was calculated for each feature, using the averaged values estimated in the study cohort as reference. The cluster with the highest number of coefficients of variation < 5% was assigned to the patient. We performed two validation approaches: firstly, a Pearson's correlation analysis was implemented to compare event frequency occurrence at 5 years in each cluster of the study cohort with those in each validation cohorts, to assess the reproducibility of TDA procedure in different settings. Second, we exploited an event-free survival analysis (Kaplan–Meier) to evaluate if the survival trend of each cluster were similar between the study cohort and the validation cohort; for this second approach, we join the internal and external validation cohort to allow a more reliable 5-year Kaplan Meyer analysis.

## Statistical analysis

For continuous variables, the Anderson–Darling test has been performed to assess the hypothesis of data normality. Continuous variables, not normally distributed were presented as median and interquartile range, while categorical data are reported as frequencies and percentages. Group comparisons for continuous and categorical variables were performed by Mann–Whitney *U* test and by chi-square ( $\chi^2$ ) test, respectively. On the hand, normally distributed variables were reported as mean  $\pm$  standard deviation and compared by unpaired t-test. The relationship between variables has been assessed by Pearson's *R* correlation coefficient. A *P*-value < 0.05 was considered statistically significant. All plots were generated by the 'ggplot2' R package. The data imputation was performed by the 'randomForest' R package.<sup>29</sup>

## Results

The analysis of the present study consists of three consecutive steps: 'step 1' was dedicated to the selection of suitable patients and features (data pre-processing), 'step 2' to unsupervised analysis for community identification, characterization and trajectory inference, and 'step 3' to a supervised analysis for risk assessment based on evaluated communities and findings validation (Figure 1).

### Step 1: Baseline characteristics of study population

Before implementing TDA, we pre-processed the original MECKI registry dataset (7948 samples and 51 clinical features) as follows: (1) features with >10% missing values were

removed; (2) samples with >5 missing values or <2-year follow-up without a MECKI outcome (non-cardiovascular death) were discarded; (3) data imputation was performed on the remaining dataset (4876 samples and 43 features) (Figure 1). Imputation was needed for 1, 2, 3, 4, and 5 parameters in 989, 429, 286, 190, and 84 patients, respectively. In 2898 patients, all 43 clinical features were available and no imputation was needed. Three hundred and ninety-nine (8%) and 789 (22%) patients reached the study endpoint at 2- and 5-year follow-up, respectively. At 5-year 1235 cases had <5 years follow-up without events. Both at 2- and 5-year follow-up patients with events were more likely male, older, with atrial fibrillation, lower blood pressure and LVEF, larger LV volumes, longer QRS duration, worst kidney function, lower haemoglobin concentration and cardiopulmonary exercise performance. As regards therapy, patients with events have a lower prescription rate of ACE/AT1/ARNI blockers but higher MRA, amiodarone and diuretic prescription (Table 1).

### Step 2: Identification and characterization of patients' communities

Based on the 43 clinical features (Table S1), TDA generated a network-based representation of the cohort with 629 nodes linked by 1088 edges, aggregating 4349 samples. Conversely 175 nodes, collecting 527 patients who, albeit with similar HF characteristics, were not closely linked to the graph; these patients were chosen as the cohort for the internal validation. Upon the network, 19 patients' communities (i.e., cluster of nodes) were, then, automatically identified (Figure 2). Interestingly, distinct sets of categorical and continuous features are predominantly associated to specific clusters (Figure 3A, B most relevant variables, Table S1 all variables and Data S1). For instance, cluster 'cl.01' and 'cl.02', albeit with a similar NYHA class ( $2.80 \pm 0.40$  and  $2.87 \pm 0.26$ , respectively), are differently characterized. The cluster 'cl.01' grouped patients with the highest frequency of exercise oscillatory ventilation (average frequency = 65%), and with the lowest values of  $VO_2$  peak % ( $32.8 \pm 6.94$ ),  $Na^+$  ( $137 \pm 1.73$ ), haemoglobin ( $11.9 \pm 0. \pm 0.9$  g/dL), and MDRD ( $43.7 \pm 13.6$  mL/min/1.73m<sup>2</sup>). On the other hand, patients belonging to the cluster 'cl.02' showed the lowest values of LVEF ( $19.4 \pm 2.01$ ),  $K^+$  ( $4.27 \pm 0.50$  meq/L) and peak exercise respiratory rate ( $29.1 \pm 3.55$ ).

### Inference of the evolution states of heart failure

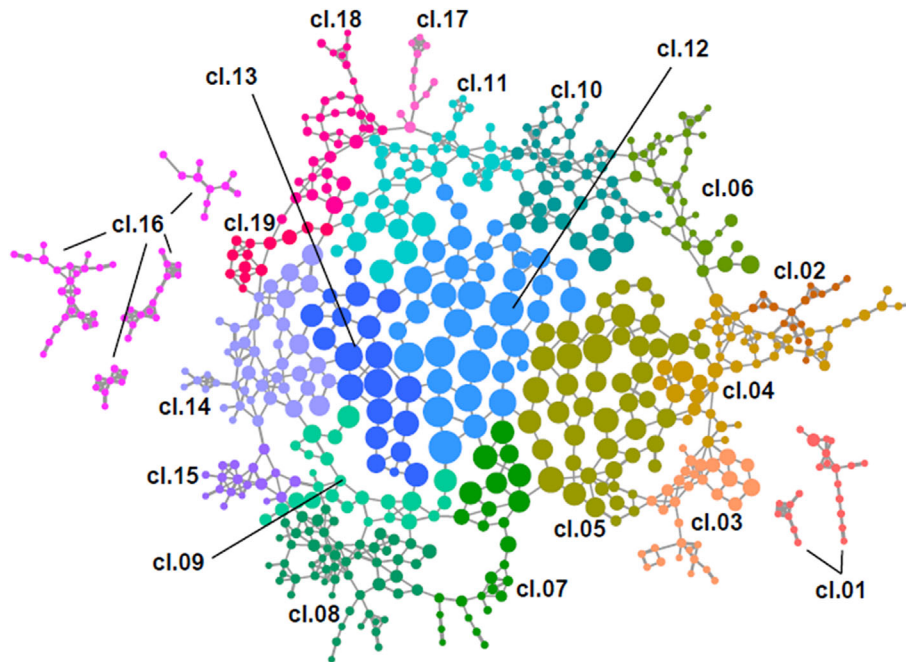
At the enrolment, HF severity of patients varied from moderate to severe. This allows hypothesizing that the clusters identified by TDA could represent specific stages of HF evolution, from the lowest to the worst severity. In addition, a trajectory analysis is able to identify all the routes connecting one or more starting

**Table 1** Collected variables according to events occurrence at 2 and 5 years follow up

	At 2 years follow-up			At 5 years follow-up		
	No event (N = 4477) (91.8%)	Event (N = 399) (8.2%)	P-value	No event (N = 2797) (78%)	Event (N = 789) (22%)	P-value
<b>General characteristics</b>						
Age (years)	63.0 [53.0, 71.0]	66.0 [55.0, 74.0]	<0.001	63.0 [53.0, 71.0]	66.0 [56.0, 74.0]	<0.001
Sex (males n, %)	3632 (81.1%)	341 (85.5%)	0.0384	2229 (79.7%)	678 (85.9%)	<0.001
BMI (kg/m <sup>2</sup> )	26.5 [24.1, 29.4]	25.4 [22.7, 28.4]	<0.001	26.6 [24.2, 29.4]	25.7 [23.1, 28.7]	<0.001
<b>Aetiology</b>						
Idiopathic (n, %)	1862 (41.6%)	145 (36.3%)	0.0985	1217 (43.5%)	281 (35.6%)	<0.001
Ischaemic (n, %)	1959 (43.8%)	195 (48.9%)	1153 (41.2%)	397 (50.3%)	43 (5.5%)	<0.001
Valvular (n, %)	213 (4.8%)	24 (6.0%)	144 (5.1%)	43 (5.5%)	144 (5.1%)	<0.001
Other (n, %)	443 (9.9%)	35 (8.8%)	283 (10.1%)	68 (8.6%)	283 (10.1%)	<0.001
LVEF (%)	33 [26, 40]	27 [23, 34]	<0.001	34 [27, 40]	28 [23, 35]	<0.001
EDV (mL)	170 [131, 210]	190 [151, 244]	<0.001	167 [129, 205]	187 [147, 237]	<0.001
ESV (mL)	109 [81, 148]	135 [101, 182]	<0.001	107 [78, 144]	130 [96, 175]	<0.001
Diastolic blood pressure (mmHg)	70 [70, 80]	70 [60, 80]	<0.001	70 [70, 80]	70 [60, 80]	<0.001
Systolic blood pressure (mmHg)	120 [105, 130]	110 [95, 120]	<0.001	120 [110, 130]	110 [100, 120]	<0.001
Rest heart rate (b.p.m.)	69 [62, 78]	72 [65, 80]	<0.001	70 [62, 78]	71 [64, 80]	<0.001
QRS duration (ms)	110 [90, 140]	120 [100, 150]	<0.001	110 [90, 134]	120 [100, 145]	<0.001
Right branch block (n, %)	254 (5.7%)	33 (8.3%)	0.0454	143 (5.1%)	63 (8.0%)	0.00293
Left branch block (n, %)	1133 (25.3%)	116 (29.1%)	0.112	774 (27.7%)	235 (29.8%)	0.263
Left anterior haemiblock (n, %)	670 (15.0%)	53 (13.3%)	0.405	421 (15.1%)	122 (15.5%)	0.82
Atrial fibrillation (n, %)	692 (15.5%)	99 (24.8%)	<0.001	430 (15.4%)	170 (21.5%)	<0.001
<b>Functional evaluation</b>						
<b>NYHA class</b>						
NYHA I (n, %)	705 (15.7%)	18 (4.5%)	<0.001	394 (14.1%)	45 (5.7%)	<0.001
NYHA II (n, %)	2698 (60.3%)	155 (38.8%)	1731 (61.9%)	355 (45.0%)	1731 (61.9%)	<0.001
NYHA III (n, %)	1027 (22.9%)	216 (54.1%)	638 (22.8%)	376 (47.7%)	638 (22.8%)	<0.001
NYHA IV (n, %)	47 (1.0%)	10 (2.5%)	34 (1.2%)	13 (1.6%)	34 (1.2%)	<0.001
VO <sub>2</sub> peak (% of predicted)	56.1 [45.1, 68.1]	41.7 [34.4, 51.6]	<0.001	56.2 [45.5, 68.0]	43.4 [36.1, 54.5]	<0.001
VO <sub>2</sub> peak (mL)	1120 [867, 1420]	835 [649, 1030]	<0.001	1120 [867, 1410]	878 [686, 1080]	<0.001
Peak heart rate (b.p.m.)	118 [102, 134]	109 [93.0, 124]	<0.001	119 [104, 136]	111 [95.0, 126]	<0.001
VE/VCO <sub>2</sub> slope	31.0 [27.0, 36.0]	37.7 [31.5, 43.1]	<0.001	30.2 [27.0, 35.0]	36.0 [30.5, 42.2]	<0.001
Respiratory exchange ratio	1.11 [1.04, 1.17]	1.09 [1.02, 1.17]	0.019	1.11 [1.03, 1.17]	1.10 [1.02, 1.17]	0.0485
Peak VE (L/min)	45.3 [36.2, 55.7]	40.5 [32.8, 50.9]	<0.001	44.4 [35.5, 54.0]	41.2 [33.9, 50.2]	<0.001
Peak workload (Watt)	80 [60, 106]	60 [49, 80]	<0.001	80 [62, 106]	66 [50, 82]	<0.001
Peak respiratory rate (b.p.m.)	31 [27, 35]	31 [27, 36]	0.221	31 [27, 35]	31 [27, 35]	0.537
Exercise oscillatory ventilation (n, %)	749 (16.7%)	126 (31.6%)	<0.001	532 (19.0%)	228 (28.9%)	<0.001
Identified anaerobic threshold (n, %)	3624 (80.9%)	270 (67.7%)	<0.001	2262 (80.9%)	558 (70.7%)	<0.001
<b>Blood samples</b>						
MDRD (mL/min/1.73 m <sup>2</sup> )	67.0 [52.5, 83.9]	54.1 [40.7, 71.9]	<0.001	69.2 [54.5, 84.6]	57.1 [42.7, 73.9]	<0.001
Haemoglobin (g/dL)	13.7 [12.5, 14.6]	12.9 [11.7, 14.0]	<0.001	13.7 [12.5, 14.6]	13.1 [11.9, 14.2]	<0.001
Creatinine (mg/dL)	1.05 [0.900, 1.28]	1.25 [1.05, 1.64]	<0.001	1.05 [0.900, 1.28]	1.20 [1.00, 1.58]	<0.001
Na <sup>+</sup> (mmol/L)	140 [138, 141]	138 [136, 141]	<0.001	140 [138, 141]	139 [136, 141]	<0.001
K <sup>+</sup> (mmol/L)	4.27 [4.00, 4.58]	4.27 [3.90, 4.60]	0.445	4.24 [4.00, 4.56]	4.23 [3.90, 4.60]	0.596
<b>Therapy</b>						
ICD (n, %)	1448 (32.3%)	201 (50.4%)	<0.001	762 (27.2%)	363 (46.0%)	<0.001
CRT (n, %)	592 (13.2%)	91 (22.8%)	<0.001	315 (11.3%)	174 (22.1%)	<0.001
Beta-blocker (n, %)	4013 (89.6%)	340 (85.2%)	0.00802	2483 (88.8%)	690 (87.5%)	0.335
ACE/ARB/ARNI (n, %)	4099 (91.6%)	327 (82.0%)	<0.001	2580 (92.2%)	671 (85.0%)	<0.001
TAO (n, %)	1320 (29.5%)	168 (42.1%)	<0.001	820 (29.3%)	306 (38.8%)	<0.001
Diuretics (n, %)	3575 (79.9%)	375 (94.0%)	<0.001	2198 (78.6%)	730 (92.5%)	<0.001
Antiplatelets (n, %)	2455 (54.8%)	211 (52.9%)	0.485	1457 (52.1%)	433 (54.9%)	0.179
MRA (n, %)	2339 (52.2%)	290 (72.7%)	<0.001	1371 (49.0%)	524 (66.4%)	<0.001
Allopurinol (n, %)	1273 (28.4%)	158 (39.6%)	<0.001	654 (23.4%)	302 (38.3%)	<0.001
Statin (n, %)	2278 (50.9%)	178 (44.6%)	0.0189	1375 (49.2%)	354 (44.9%)	0.0365
Amiodarone (n, %)	1000 (22.3%)	152 (38.1%)	<0.001	608 (21.7%)	270 (34.2%)	<0.001
Digitalis (n, %)	764 (17.1%)	119 (29.8%)	<0.001	527 (18.8%)	227 (28.8%)	<0.001
<b>Cardiovascular events</b>						
Cardiovascular death (n, %)	-	314 (78.7%)	-	-	645 (81.7%)	-
Heart transplant (n, %)	-	64 (16.0%)	-	-	112 (14.2%)	-
LVAD (n, %)	-	21 (5.3%)	-	-	32 (4.1%)	-

ACE, angiotensin converting enzyme; ARB, angiotensin receptor blockers; ARNI, angiotensin receptor-neprilysin inhibitor; BMI, body mass index; CRT, cardiac resynchronization therapy; EDV, end-diastolic volume; ESV, end-systolic volume; ICD, implantable cardioverter defibrillator; LVAD, left ventricular assist device; LVEF, left ventricular ejection fraction; MDRD, glomerular filtration rate with modification of diet in renal disease formula; MRA, mineralocorticoid receptor antagonist; NYHA, New York Heart Association class; VE, ventilation; VE/VCO<sub>2</sub> slope, minute ventilation/carbon dioxide production relationship slope; VO<sub>2</sub> peak, oxygen uptake at peak exercise.

**Figure 2** Cluster identification by topological data analysis. Each node of the network represents a group of patients. The node size is proportional to the number of enclosed samples, while edges thickness depicts the Jaccard's index (i.e., the number of samples shared by nodes). Each identified cluster has been highlighted with different colors.



clusters to several endpoint clusters. This necessarily implies that the pathways (i.e., the disease evolution) in some clusters can follow at least two different directions. We referred to those clusters as 'bifurcation points'. Here, by the trajectory analysis, a path was identified (*Figure 4A*), starting from cluster 'cl.16' (average pseudo-time:  $2.8 \pm 2.6$ ). In the HF evolution path, 3 bifurcation points (red squares) at clusters 'cl.13' (pseudo-time:  $8.1 \pm 1.9$ ), 'cl.09' (pseudo-time:  $10.1 \pm 1.3$ ), and 'cl.07' (pseudo-time:  $12.8 \pm 1.4$ ) were identified. Finally, 4 stopping points (yellow diamonds) at clusters 'cl.15' (pseudo-time:  $9.1 \pm 0.9$ ), 'cl.06' (pseudo-time:  $14 \pm 3.4$ ), 'cl.01' (pseudo-time:  $17 \pm 0.8$ ), and 'cl.02' (pseudo-time:  $18 \pm 0.8$ , *Figure 4B* and *Figure S1*) ended the HF evolution trajectory. The stopping points can be considered specific end-stages of the disease and are associated to peculiar characteristics (*Table 2*) and patients' prognosis. Indeed, the 2-year study endpoint prevalence was 56%, 36%, 9%, and 2%, the 5-year study endpoint prevalence was 73.5%, 60%, 25%, and 6%, while average MECKI score at enrolment was 20%, 13%, 11%, and 10% for cluster 'cl.01', 'cl.02', 'cl.06', and 'cl.15', respectively.

Differently, the bifurcation points represent key states to determine distinct disease evolutions; therefore, we identified the features that are significantly different comparing the samples belonging to the bifurcation point with those in the adjacent clusters (*Table 3*). In *Table 3*, the bifurcation cluster is reported in the middle while on the left and right the less and more adverse evolution, respectively. For example, for patients in cluster 'cl.13' a negative HF evolution, that is,

evolution to cluster 'cl.09', is foreseen for patients who develop atrial fibrillation, increase NYHA class, reduces kidney function and peak  $VO_2$  with a simultaneous increase of the  $VE/VCO_2$  slope while a more favourable evolution, that is, to cluster 12, is foreseen for patients who had a higher QRS duration, underwent a pacemaker therapy and had a more frequent MRA treatment. Similarly, at the second bifurcation, that is, 'cl.09', a negative HF evolution is expected in patients who reduced BMI, haemoglobin, kidney function and increase resting heart rate and frequency of exercise induced oscillatory breathing; differently a less negative evolution is suggested by the presence of reduced digitalis, MRA therapy and ICD, higher LVEF and short QRS. At the third bifurcation a negative HF evolution is foreseen in patients with increase in heart rate and NYHA class as well as a decrease in  $K^+$ ,  $NA^+$  level, and  $VO_2$  peak % as these patients will follow the route through the 'cl.01' end-stage; differently, patients following the other route ('cl.02' end-stage) showed a significant increase of haemoglobin levels ( $P < 0.001$ ).

### Step 3: Survival analysis and MECKI study endpoint (cardiovascular death, urgent heart transplant, or left ventricular assist device) by communities

So far, we identified HF patients' communities in an unsupervised way, that is, without knowing any disease outcomes.

**Figure 3** Clusters characterization. (A) The bubble plot represents the average frequency of samples exhibiting a specific categorical feature (y-axis) in each cluster (x-axis); the higher the circle, the higher the sample rate. (B) The bubble plot represents the distribution of continuous variables (min-max scaling); the higher the circle size, the higher the average feature value in a specific cluster. All frequencies, means and standard deviations of each feature for each cluster are present in *Table S1*.

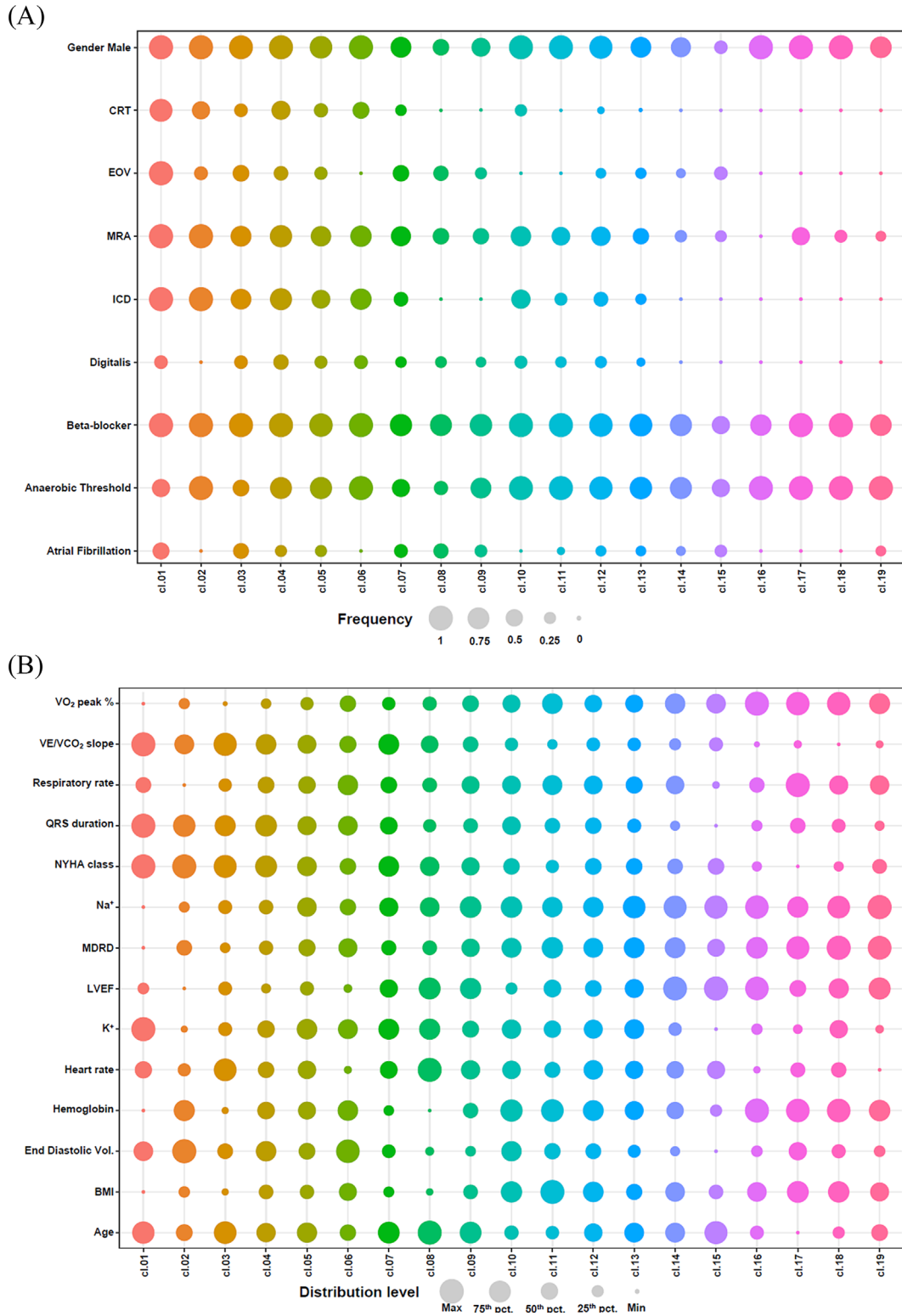
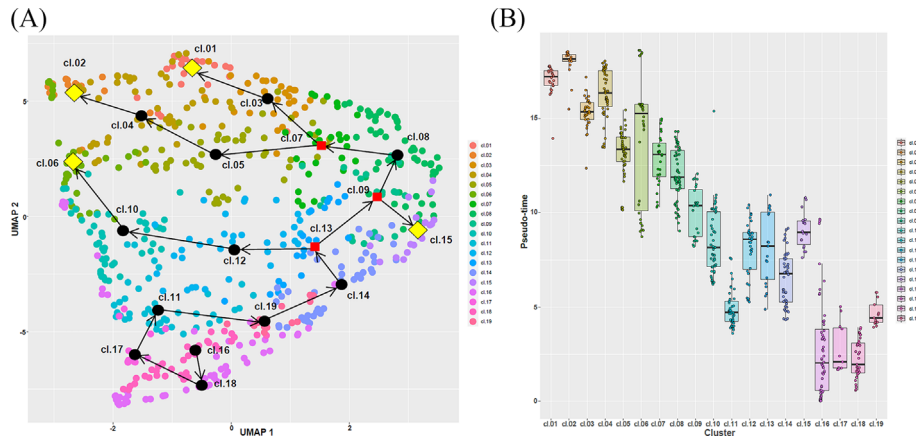


**Figure 4** Trajectory Analysis. (A) The dot plot shows the UMAP representation of TDA network nodes which allowed to infer cluster centroids (red squares for bifurcation points, yellow diamonds for stopping point and black circles for all other clusters) and to identify the most likely trajectories between clusters. The arrows depict the HF evolution albeit a reverse evolution is possible as shown in Figure S3A, B. (B) The boxplot represents the distribution of pseudo-time estimated for each cluster; dots represent the pseudo-time value calculated for each TDA node.



However, the MECKI registry recorded also a prolonged follow-up. Therefore, we performed a survival analysis, stratifying data by communities. Interestingly, 'cl.01' and 'cl.02', which were also identified as end-stages in the trajectory analysis, showed the lowest survival rate at 2 (44.1% and 62.5%) and 5 year (20% and 35.2%, respectively). On the other hand, patients belonging to 'cl.11', 'cl.12', 'cl.13', 'cl.14', 'cl.15', 'cl.16', 'cl.17', 'cl.18', and 'cl.19' (the first stages in trajectory analysis) showed a survival rate higher than 90% at a 5-year follow-up (Figure 5A). In addition, we confirmed that each cluster can be considered as a specific state of heart failure progression, exploiting the blood concentrations of B-Type Natriuretic Peptide (BNP), a well-known biomarker of Heart Failure severity,<sup>30</sup> available at the baseline for 2840 patients (58%) and therefore not included in the initial analysis. A Pearson's correlation analysis highlighted a relevant negative relationship ( $R = -0.96$ ,  $P < 0.001$ ) between the average concentrations of BNP with the event-free survival rates at 5 years of each cluster (Figure S2). It is acknowledged that we have not considered NTproBNP but BNP only. Indeed, NTproBNP was available only in 1085 cases. Moreover, we have not included in the present subanalysis patients on ARNI treatment due to the direct influence of ARNI on BNP value.

### Validation

To confirm that reliability of our finding we performed an internal and an external validation study. To do so, we inferred the cluster membership for the 527 patients of the internal validation cohort and 777 of the external validation cohort (Figure 1). Interestingly, the percentage of events in each cluster for both the validation cohorts is highly correlated to that of the study cohort, being the Pearson's correlation index  $R = 0.94$  ( $P < 0.001$ , Figure 6A) and  $R = 0.84$  ( $P < 0.001$ , Figure 6B), when comparing the internal and

the external validation cohort, respectively. Of note, the survival analysis was performed grouping patients according the 19 clusters and considering the HF population of the two validation cohorts combined ( $n = 1304$ ). The results were comparable with those of the original study population (Figure 5B and Data S1); indeed, comparing the Kaplan–Meier curves trend for each cluster in both cohorts, we confirmed that there no significant difference between any cluster ( $P > 0.05$ ), except cluster 'cl.06' (Figure S3).

Looking deeper into the difference between the 'cl.06' in both cohorts, we confirmed that the high majority of variables are not statistically different. However, we noted in the validations cohort a significant increase of the average rest heart rate (74.7 vs. 68.1 b.p.m.), and of the atrial fibrillation patients' frequency (32% compare to 4% in study population). Moreover, survival differences between the two 'cl.06' cohorts are mainly related to the first year (Figure S1).

## Discussion

In the present study, utilizing a dedicated analytical approach, we showed that HF progression is characterized by a continuous but heterogeneous evolution process. The HF evolution leads to four terminal stages differentiated as for characteristics and prognosis. During HF progression, patients meet 3 bifurcation points, which determine HF evolution and outcome. Accordingly, special attention needs to be dedicated to patients when their HF trajectory reaches a bifurcation point since the subsequent evolution leads to a different outcome. Of note, albeit HF is usually seen as a progressive disease<sup>31</sup> internodes trajectories are potentially bidirectional with a reverse direction in case of HF recovery.

**Table 2** Feature distributions for end stage clusters

	cl.01	cl.02	cl.06	cl.15
No. of nodes	(N = 22)	(N = 17)	(N = 34)	(N = 18)
No. of patients	(n = 34)	(n = 24)	(n = 123)	(n = 49)
Age (years)	68.7 ± 7.19	56.5 ± 8.54	54.8 ± 8.67	71.5 ± 5.79
Sex (males %)	92.8 ± 23.3	100	97.9 ± 5.42	24.3 ± 27.6
BMI (kg/m <sup>2</sup> )	24.6 ± 3.28	26.2 ± 4.25	27.2 ± 2.32	26.2 ± 2.48
Idiopathic aetiology (%)	63.6 ± 49.2	76.5 ± 43.7	70.6 ± 46.2	0
Ischaemic aetiology (%)	36.4 ± 49.2	23.5 ± 43.7	29.4 ± 46.2	5.6 ± 23.6
Valvular aetiology (%)	0	0	0	38.9 ± 50.2
Other aetiology (%)	0	0	0	55.6 ± 51.1
LVEF (%)	23.4 ± 4.67	19.4 ± 2.01	21.8 ± 3.42	50.3 ± 3.57
EDV (mL)	254 ± 55.5	356 ± 45.5	335 ± 57.3	88.7 ± 14.3
ESV (mL)	188 ± 36.3	287 ± 38.4	259 ± 53.2	48.0 ± 12.3
Diastolic blood pressure (mmHg)	63.0 ± 4.69	61.2 ± 5.27	68.7 ± 5.95	77.9 ± 4.93
Systolic blood pressure (mmHg)	92.8 ± 6.83	100 ± 13.0	110 ± 9.68	132 ± 12.2
Rest heart rate (b.p.m.)	71.2 ± 13.6	70.8 ± 10.2	68.1 ± 6.27	71.3 ± 7.76
Right branch block	1.05 ± 4.92	0	2.71 ± 7.55	11.7 ± 24.5
Left branch block	38.8 ± 36.6	33.4 ± 35.9	46.8 ± 25.4	2.56 ± 6.55
Left anterior haemoblock	7.46 ± 16.7	0	9.6 ± 13.5	8.41 ± 11.9
QRS duration (ms)	164 ± 16.7	152 ± 21.2	137 ± 17.3	86.4 ± 9.99
Atrial fibrillation (%)	43.1 ± 41	22 ± 29.3	4.82 ± 11.2	21.1 ± 25.1
NYHA class	2.80 ± 0.378	2.87 ± 0.265	2.07 ± 0.384	1.91 ± 0.221
VO <sub>2</sub> peak (% of predicted)	32.8 ± 6.94	41.4 ± 5.38	55.0 ± 7.74	70.3 ± 11.6
VO <sub>2</sub> peak (mL)	637 ± 127	1010 ± 97.5	1290 ± 164	947 ± 100
VE/VCO <sub>2</sub> slope	43.5 ± 7.13	37.3 ± 4.45	33.3 ± 3.27	30.6 ± 1.85
Peak heart rate (b.p.m.)	88.2 ± 17.7	106 ± 14.6	116 ± 10.9	125 ± 19.3
Respiratory exchange ratio	1.10 ± 0.109	1.12 ± 0.0850	1.14 ± 0.0819	1.05 ± 0.0395
Peak VE (L/min)	37.0 ± 6.61	48.9 ± 6.48	52.5 ± 7.25	33.1 ± 3.56
Peak workload (Watt)	41.5 ± 10.7	69.9 ± 8.37	91.1 ± 12.2	72.1 ± 17.9
Peak respiratory rate (b.p.m.)	30.2 ± 3.64	29.1 ± 3.55	33.2 ± 5.39	29.3 ± 3.06
Exercise oscillatory ventilation (%)	65.4 ± 42.2	29.9 ± 33.2	13 ± 18.7	25.8 ± 25.7
Identified anaerobic threshold (%)	42.6 ± 37.9	88.5 ± 19.8	96.4 ± 7.08	43.9 ± 29.8
MDRD (mL/min/1.73 m <sup>2</sup> )	43.7 ± 13.6	57.0 ± 12.7	70.3 ± 13.8	64.7 ± 11.2
Haemoglobin (g/dL)	11.9 ± 0.909	13.8 ± 0.909	14.0 ± 0.759	12.5 ± 0.538
Creatinine (mg/dL)	1.81 ± 0.442	1.29 ± 0.249	1.13 ± 0.170	1.06 ± 0.119
Na <sup>+</sup> (mmol/L)	137 ± 1.73	138 ± 3.12	138 ± 2.21	140 ± 1.31
K <sup>+</sup> (mmol/L)	4.46 ± 0.383	4.27 ± 0.505	4.29 ± 0.229	4.10 ± 0.197
ICD (%)	92.3 ± 23.5	86.3 ± 26.8	72.6 ± 25.8	0
CRT (%)	74.6 ± 29.2	67 ± 34.3	50.4 ± 26.4	0
Beta-blocker (%)	91.7 ± 23.6	97.6 ± 6.64	95.7 ± 8.97	56.7 ± 26
ACE/ARB/ARNI (%)	68.5 ± 36	92.4 ± 17.1	95.7 ± 8.83	83.5 ± 22
TAO (%)	70.2 ± 33.3	48.5 ± 42.5	46.9 ± 30.1	35.9 ± 28.9
Diuretics (%)	100	100	94.3 ± 11.2	50.3 ± 35.2
Antiplatelets (%)	28.7 ± 36.5	40.8 ± 38.1	41.8 ± 26.6	53.2 ± 28.3
MRA (%)	75.3 ± 36.2	86.7 ± 19.7	75.2 ± 22.9	19.7 ± 26
Allopurinol (%)	54.1 ± 40.6	74.7 ± 24.5	31.1 ± 30.4	4.21 ± 7.41
Statin (%)	27.5 ± 37.6	25.5 ± 30.9	32.1 ± 30.7	54.8 ± 29.3
Amiodarone (%)	70.1 ± 35	58 ± 37.7	37.6 ± 28.7	3.39 ± 6.76
Digitalis (%)	33.2 ± 38.1	26.9 ± 31.9	33 ± 30.1	7.42 ± 10.4

Each element of the table expresses the mean (±standard deviation) of the variable in a specific cluster. To calculate this mean, we computed the overall mean of the nodes in the cluster, which, in turn, is the average of patients belonging to a specific node.

ACE, angiotensin converting enzyme; ARB, angiotensin receptor blockers; ARNI, angiotensin receptor-neprilysin inhibitor; BMI, body mass index; CRT, cardiac resynchronization therapy; EDV, end-diastolic volume; ESV, end-systolic volume; ICD, implantable cardioverter defibrillator; LVAD, left ventricular assist device; LVEF, left ventricular ejection fraction; MDRD, glomerular filtration rate with modification of diet in renal disease formula; MRA, mineralocorticoid receptor antagonist; NYHA, New York Heart Association class; VE, ventilation; VE/VCO<sub>2</sub> slope, minute ventilation/carbon dioxide production relationship slope; VO<sub>2</sub> peak, oxygen uptake at peak exercise.

The study population was sizable with several variables derived from anthropometric, clinical, laboratory, therapy, cardiac ultrasound, and cardiopulmonary exercise testing data. Each of the analyzed variable has a recognized and frequently independent prognostic role in chronic HF. The study patients' population was recruited by a large number of HF centres. Patients had mostly moderate HF based on survival, NYHA class, exercise performance, cardiac volumes and LVEF, kidney func-

tion, haemoglobin levels, blood pressure and incidence of atrial fibrillation. Of note, to be eligible patients were required to have a history of HF with reduced LVEF, but this condition could not be present at the time the CPET was performed. Treatment was optimized in accordance with HF guidelines in place at study time. As a matter of fact, beta-blockers, angiotensin converting enzyme inhibitors/angiotensin receptor blockers/angiotensin receptor-neprilysin inhibitor (ARNI), and

mineralocorticoid receptor antagonist were prescribed in a relevant fraction of patients as were ICD and CRT devices.

We required the existence of >2 years follow-up as in the original MECKI algorithm and assessed patients' prognosis up to 5 years. Indeed, for a HF population with mostly moderate HF, a 2- and 5-year timeframe seems to us a reasonable length of time, being a shorter interval more appropriate for patients with more severe HF and a longer one not particularly relevant due to several possible intercurrent confounding events. Consequently, albeit the continuous updating of the MECKI database, we evaluated patients recruited up to 2020, while patients recruited afterwards were not considered in the present analysis. We recognize that this period was arbitrary and that potential prognostic benefit of new HF drugs such as gliflozins and ARNI was therefore not considered or limited, respectively. Accordingly, a further re-evaluation of HF trends will be needed after the widespread and more prolonged introduction of those drugs as suggested by 2021 ESC guidelines.<sup>2</sup>

In the era of precision medicine, a relevant unmet need is still the accurate identification of homogeneous subgroups of patients in heterogeneous cohorts<sup>4</sup>; this is, particularly evident for the heart failure.<sup>32</sup> Today, many unsupervised artificial intelligence techniques could help face this issue<sup>33</sup>; one of these, the TDA, has proved to be an effective in identify sub-phenotypes of patients in cardiovascular settings. Indeed, the TDA has been recently used for phenotyping patients with diabetes and aortic stenosis as well as to describe the evolution of coronary artery diseases.<sup>15,34,35</sup>

In the present study, we applied an unsupervised topology-based approach to identify HF patients' clusters with peculiar characteristics and estimate HF evolution; indeed, exploiting the pseudo-time estimation, an established technique to estimate the cell fate evolution in single cell RNA-Seq data, we inferred the continuous progression of HF disease states, assuming a cluster as a disease stage. The pseudo time analysis allows to evaluate in a comparable fashion the evolution speed of the different HF settings. Overall and most importantly, we showed that HF progression is characterized by a continuous but heterogeneous evolution process in which many bidirectional trajectories, both toward a disease progression but also toward recovery, are conceivable.

Specifically, the TDA allowed the identification of 19 groups of patients with peculiar clinical characteristics and the identification of possible path of HF evolution. Indeed, it is important to identify the cluster to which the patient belong both to precisely define his/her prognosis but also to understand in which direction the disease is evolving. In addition, we described that the HF progression leads to four terminal clusters associated with different characteristics and prognosis. For instance, comparison of 'cl.01' and cl.02, showed albeit a similar NYHA class a different phenotype with highest frequency of exercise oscillatory ventilation, lowest values of haemoglobin, peak VO<sub>2</sub> and kidney function

in the former and a lower LVEF in the latter suggesting a mainly 'peripheral' phenotype in 'cl.01' and 'central' in 'cl.02'. Moreover, during HF progression, patients encounter 3 bifurcation points, which determine distinct HF evolution and outcome. Accordingly, special attention needs to be dedicated to patients when their HF trajectory reaches a bifurcation point since the subsequent evolution leads to a different outcome. Therefore, the identification of a cluster which has multiple evolution paths is of relevant clinical impact. Of note, albeit HF is usually seen as a progressive disease,<sup>31</sup> internodes trajectories are potentially bidirectional with a reverse direction in case of HF recovery.

The present cluster analysis was validated considering an internal cohort of 527 patients. These patients were recruited in the same time period of the original study population and a relevant concordance between events was observed. A second validation cohort ( $n = 777$ ) was obtained from the MECKI international registry<sup>28</sup> and again a relevant concordance between events was observed. Of note, the two implemented validation analysis confirmed the reproducibility of our results. All together, these findings imply that the phenotyping of patients in 19 clusters is reliable as regards events. Clearly further validations are needed particularly since a few new, effective, disease modifying drugs have been introduced as new is the therapeutic approach of the latest guidelines. On this regards it is of note that, applying the present analysis to data derived from a recently published paper on MECKI score reassessment<sup>1</sup> where patients were evaluated twice, we ascertained that either patients, who improved (23.7% of tested patients) or worsened (40% of tested patients) the MECKI score, followed the above described HF trajectories (Figure S4A). Moreover, in another experimental settings, where patients, not included in the main study and with a short follow-up, were evaluated before and after ARNI ( $n = 47$ ) or dapagliflozin ( $n = 19$ ) treatment, we observed that all patients who improved their condition (43.4%), followed backward the HF trajectories (Figure S4B). Again, these findings albeit very preliminary, reinforce the reliability of the present analysis. Consequently, we believe that the application of our or similar HF evolution models will allow a more comprehensive patients phenotyping, a more appropriate patients management and consequently resource allocation. Indeed, the patients at the bifurcation points seems to us those who need a stricter follow up being at a point where the evolution path may change.

The present investigation suffers of a few limitations, which need to be acknowledged. First, we analysed only patients with history of low LVEF. Hence, patients with preserved and mildly reduced LVEF have not been tested systematically. Second, the number of female HF patients, 903 (19.0%) and 679 (18.9%) at 2- and 5-year follow-up, respectively was relatively small and not tested independently. Similarly, the great majority of our patients were Caucasian, so that we do not know how the present model performs

**Table 3** Variables means in bifurcation points

	First bifurcation (cl.13)				
	cl.12 (N = 36) (n = 717)	cl.13 (N = 20) (n = 359)	cl.09 (N = 24) (n = 236)	P-value (cl.12 vs. cl.13)	P-value (cl.09 vs. cl.13)
BMI (kg/m <sup>2</sup> )	27.8 ± 0.746	26.7 ± 0.892	26.3 ± 0.984	<0.001	0.156
Atrial fibrillation (%)	14.1 ± 7.46	12.8 ± 5.75	23.9 ± 19.6	0.464	<b>0.006</b>
NYHA class	1.99 ± 0.173	2.03 ± 0.121	2.18 ± 0.123	0.34	<0.001
VO <sub>2</sub> peak (% of predicted)	59.4 ± 5.02	60.9 ± 6.50	55.6 ± 5.56	0.389	<b>0.002</b>
VE/VCO <sub>2</sub> slope	30.2 ± 1.59	30.1 ± 1.46	32.8 ± 2.07	0.85	<0.001
MDRD (mL/min/1.73 m <sup>2</sup> )	71.6 ± 4.12	74.2 ± 5.29	67.0 ± 8.07	0.069	<0.001
Na <sup>+</sup> (mmol/L)	139 ± 0.501	140 ± 0.501	140 ± 1.29	<b>0.002</b>	0.328
QRS duration (ms)	116 ± 5.95	107 ± 6.58	107 ± 10.6	<0.001	0.974
MRA (%)	59.6 ± 11.4	40.3 ± 11.6	40.9 ± 17.8	<0.001	0.892
	Second bifurcation (cl.09)				
	cl.15 (N = 18) (n = 49)	cl.09 (N = 24) (n = 236)	cl.08 (N = 56) (n = 191)	P-value (cl.15 vs. cl.09)	P-value (cl.08 vs. cl.09)
BMI (kg/m <sup>2</sup> )	26.2 ± 2.48	26.3 ± 0.984	25.2 ± 2.30	0.585	<b>0.005</b>
LVEF (%)	50.3 ± 3.57	41.6 ± 5.63	44.2 ± 7.26	<0.001	0.085
QRS duration (ms)	86.4 ± 9.99	107 ± 10.6	101 ± 15.3	<0.001	0.052
Peak heart rate (b.p.m.)	71.3 ± 7.76	71.0 ± 3.10	74.6 ± 6.97	0.78	<b>0.011</b>
Peak respiratory rate (b.p.m.)	29.3 ± 3.06	31.4 ± 1.67	30.5 ± 3.78	<b>0.0133</b>	0.132
Exercise oscillatory ventilation (%)	25.8 ± 25.7	21.2 ± 14.2	35.5 ± 26	0.759	<b>0.0107</b>
Haemoglobin (g/dL)	12.5 ± 0.538	12.8 ± 0.495	11.9 ± 0.722	0.078	<0.001
MDRD (mL/min/1.73 m <sup>2</sup> )	64.7 ± 11.2	67.0 ± 8.07	54.8 ± 11.7	0.465	<0.001
ICD (%)	0	5.19 ± 9.45	4.08 ± 8.54	<b>0.002</b>	0.173
MRA (%)	19.7 ± 26	40.9 ± 17.8	39.2 ± 29.7	<b>0.006</b>	0.67
Digitalis (%)	7.42 ± 10.4	15.1 ± 12.4	14.2 ± 13.1	<b>0.03</b>	0.835
	Third bifurcation (cl.07)				
	cl.05 (N = 49) (N = 761)	cl.07 (N = 27) (n = 235)	cl.03 (N = 32) (n = 156)	P-value (cl.05 vs. cl.07)	P-value (cl.03 vs. cl.07)
Atrial fibrillation (%)	16.8 ± 7.22	33.2 ± 28.1	34.7 ± 24.5	<b>0.003</b>	0.437
NYHA class	2.39 ± 0.219	2.46 ± 0.259	2.79 ± 0.241	0.199	<0.001
VO <sub>2</sub> peak (% of predicted)	45.6 ± 4.63	42.7 ± 8.53	32.9 ± 4.68	0.27	<0.001
Peak heart rate (b.p.m.)	70.8 ± 2.41	69.3 ± 4.68	74.1 ± 7.51	0.17	<b>0.003</b>
Exercise oscillatory ventilation (%)	22.1 ± 9.55	39.8 ± 25.1	45.7 ± 27	<b>0.002</b>	0.391
Haemoglobin (g/dL)	13.3 ± 0.490	12.2 ± 0.762	11.9 ± 0.948	<0.001	0.259
Na <sup>+</sup> (mmol/L)	139 ± 0.649	139 ± 1.47	138 ± 1.36	0.786	<b>0.009</b>
K <sup>+</sup> (mmol/L)	4.32 ± 0.111	4.33 ± 0.151	4.20 ± 0.233	0.789	<b>0.011</b>

Each element of the table expresses the mean (±standard deviation) of the variable in a specific cluster. To calculate this mean, we computed the overall mean of the nodes in the cluster, which, in turn, is the average of patients belonging to a specific node. Data in bold indicate  $P < 0.05$ .

ACE, angiotensin converting enzyme; ARB, angiotensin receptor blockers; ARNI, angiotensin receptor-neprilysin inhibitor; BMI, body mass index; CRT, cardiac resynchronization therapy; EDV, end-diastolic volume; ESV, end-systolic volume; ICD, implantable cardioverter defibrillator; LVAD, left ventricular assist device; LVEF, left ventricular ejection fraction; MDRD, glomerular filtration rate with modification of diet in renal disease formula; MRA, mineralocorticoid receptor antagonist; NYHA, New York Heart Association class; VE, ventilation; VE/VCO<sub>2</sub> slope, minute ventilation/carbon dioxide production relationship slope; VO<sub>2</sub> peak, oxygen uptake at peak exercise.

in other races. Third, albeit we analyzed several variables some of those known to have an impact on HF prognosis such as sleep disorders, genetics and family history, prevalence of catheter ablation for atrial fibrillation or cardiac rehabilitation were not considered. On this regard, BNP, probably the most used HF prognostic and diagnostic biomarker was not included in the present analysis because available only in 2840 out of 4348 cases. Indeed, in the early cases BNP measurement was not routinely performed in all centers and, in the most recent cases only NT-proBNP was available. Of note, in each cluster BNP value was strongly associated with the

5-year event free survival rate (Figure S2) supporting the consistency of the implemented unsupervised approach. Fourth, the effect of treatment changes or of events needs to be assessed in larger populations. Indeed, the few cases we analysed (Figure S4A, B) are just a tentative and should be seen as a work in progress and a very preliminary analysis which needs to be confirmed. Fifth, patients' recruitment period was large, expanding from 1993 to 2022, a period during which significant advancement in treatment modalities and diagnostic features happened. However, we assessed the impact of time of patients recruitment on our findings enriching

**Figure 5** Survival analysis. (A) The Kaplan–Meier curve of the study population with the event-free survival for each cluster at 5-year follow-up. (B) The Kaplan–Meier curve of the two validation cohorts combined.

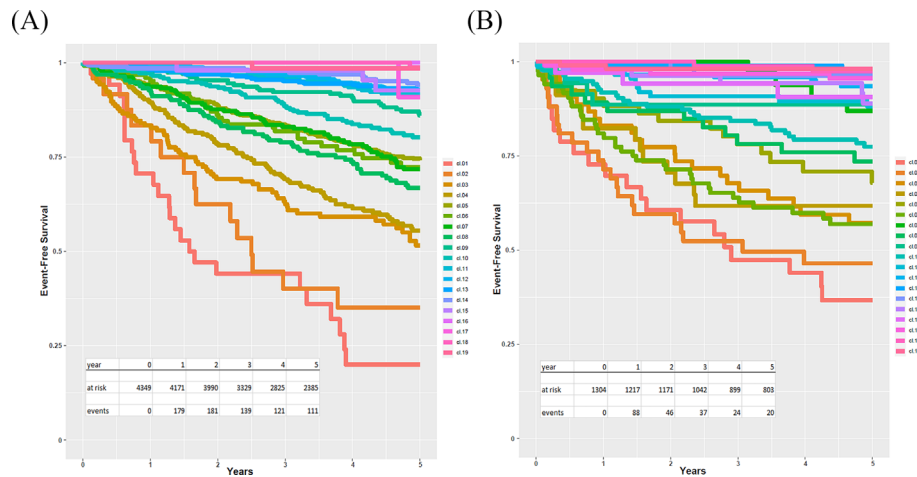
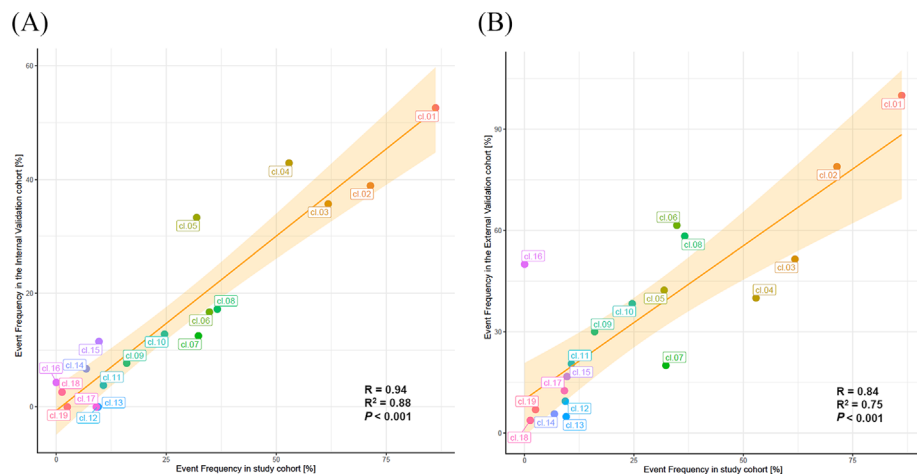


**Figure 6** Validation analysis. (A) The scatter plot shows the correlation between the frequency of study endpoints at 5 years within each cluster in the study population (x-axis) and in the internal validation cohort (y-axis). (B) The same plot is shown to correlate frequency of study endpoints at 5 years, even with the external validation cohort (y-axis). For both the correlation analysis, the Pearson's correlation coefficient ( $R$ ) and the relative  $P$ -value were computed to evaluate the strength of association between the two methodologies. The 95% confidence interval of the trendline (orange line) is depicted in light orange.



the TDA network using the time of enrollment, and found no influence.

Furthermore, it must be recognized that the present HF evolution model needs to be tested and validated by an independent revision. As a matter of facts, a sequential assessment of clinical data was not available so that the real heart failure progression paths still need to be evaluated. Indeed, although we believe that the present approach represents a relevant step forward in the evaluation of HF management it must be recognized that a perfect prognostic algorithm is still unreached and a continuous update involving more patients with different HF phenotypes and therapies is mandatory. In other

words, HF prognosis evaluation is an endless story which remember to me a famous poem ... *espera luz espera, Y corro ansioso loco. Espera luz espera, Y cuando voy a legar a su lado, se oscurece, fria, ...* (Juan Ramón Jiménez).

## Research in the context

This study, leveraging TDA on a cohort of 4876 chronic heart failure (HF) patients, identified 19 distinct HF phenotypes with unique progression trajectories. Crucially, bifurcation points and stopping points were showed, signifying pivotal junctures

and end-stage conditions, respectively. Survival rates varied significantly among clusters, offering a nuanced understanding of HF prognosis. The robust validation of findings in internal and external cohorts reinforces the clinical applicability of our approach, providing a foundation for personalized HF patient management.

Our findings redefine the landscape of HF prognostication, offering a novel framework for tailoring assessments to individual patients. The identified bifurcation points highlight critical decision junctures, necessitating focused clinical attention. Looking forward, this work paves the way for future research into targeted interventions at these key points, aiming to improve outcomes and reshape the management of chronic HF. The identified phenotypes serve as a foundation for developing precision medicine approaches in HF care, emphasizing the potential for more effective and individualized treatment strategies. Moreover, the described HF evolution pathways may be reverted in case of therapeutic intervention. The latter needs to be validated by further larger studies.

## Funding

The study was supported by Italian Ministry of Health (Ricerca Corrente; CUP=B43C24000090001).

## Acknowledgements

Open access funding provided by BIBLIOSAN. [Correction added on 27 September 2024, after first online publication: BIBLIOSAN funding statement has been added.]

## Conflict of interest

None declared.

## References

1. Pezzuto B, Piepoli M, Galotta A, Sciomer S, Zaffalon D, Filomena D, *et al.* The importance of re-evaluating the risk score in heart failure patients: An analysis from the metabolic exercise cardiac kidney indexes (MECKI) score database. *Int J Cardiol* 2023;**376**:90-96. doi:10.1016/j.ijcard.2023.01.069
2. McDonagh TA, Metra M, Adamo M, Gardner RS, Baumbach A, Bohm M, *et al.* 2021 ESC guidelines for the diagnosis and treatment of acute and chronic heart failure. *Eur Heart J* 2021;**42**:3599-3726. doi:10.1093/eurheartj/ehab368
3. Agostoni P, Corra U, Cattadori G, Veglia F, La Gioia R, Scardovi AB, *et al.* Metabolic exercise test data combined with cardiac and kidney indexes, the MECKI score: A multiparametric approach to heart failure prognosis. *Int J Cardiol* 2013;**167**:2710-2718. doi:10.1016/j.ijcard.2012.06.113
4. Leopold JA, Loscalzo J. Emerging role of precision medicine in cardiovascular disease. *Circ Res* 2018;**122**:1302-1315. doi:10.1161/CIRCRESAHA.117.310782
5. Campodonico J, Nicoli F, Motta I, Migone De Amicis M, Bonomi A, Cappellini M, *et al.* Prognostic role of transferrin saturation in heart failure patients. *Eur J Prev Cardiol* 2021;**28**:1639-1646. doi:10.1093/eurjpc/zwaa112
6. Ferreira JP, Verdonschot J, Collier T, Wang P, Pizard A, Bar C, *et al.* Proteomic bioprofiles and mechanistic pathways of progression to heart failure. *Circ Heart*

## Data availability statement

Repository of raw data will be available after acceptance at [www.zenodo.org](http://www.zenodo.org).

## Supporting information

Additional supporting information may be found online in the Supporting Information section at the end of the article.

**Figure S1.** Evolution states of HF by pseudo-time analysis. As in Figure 4A the dot plot shows the UMAP representation of TDA network nodes with pseudo time analysis. For symbols see Figure 4A.

**Figure S2.** BNP analysis. Linear correlation between BNP (log) vs. 5 year survival defined as the composity of cardiovascular death, urgent heart transplant or LVAD implantation.

**Figure S3.** Survival analysis. Kaplan Meyer curves in each cluster comparing the study population and the 2 validation cohorts combined. The study endpoint was the combination of cardiovascular death, urgent heart transplant or LVAD.

**Figure S4.** Tentative application of TDA in clinical settings. A) A first tentative application of our finding in a cohort of patients who repeating CPET after 1–2 years from the first examination.<sup>1</sup> As expected, most of samples worsened (40%, red arrows) during time, following the route we identified in trajectory analysis, while a few of them improved their condition (23.7%; blue arrows). B) A second tentative application in a small cohort of samples who repeated CPET after 6–9 months treated with ARNI or dapagliflozin. About half (56.6%) of samples did not change their condition while all the other improved their status (43.4%; blue arrows). In both diagrams, each node represent the cluster centroid as in Figure 4A, while arrows could have specific direction whether patients improve (blue arrows) or worsen (red arrow) their condition.

**Table S1:** feature distributions for each cluster.

**Data S1.** Supporting Information.

- Fail* 2019;**12**:e005897. doi:10.1161/CIRCHEARTFAILURE.118.005897
7. Hage C, Michaelsson E, Linde C, Donal E, Daubert JC, Gan LM, *et al.* Inflammatory biomarkers predict heart failure severity and prognosis in patients with heart failure with preserved ejection fraction: A holistic proteomic approach. *Circ Cardiovasc Genet* 2017;**10**:doi:10.1161/CIRCGENETICS.116.001633
  8. Aaronson KD, Schwartz JS, Chen TM, Wong KL, Goin JE, Mancini DM. Development and prospective validation of a clinical index to predict survival in ambulatory patients referred for cardiac transplant evaluation. *Circulation* 1997;**95**:2660-2667. doi:10.1161/01.cir.95.12.2660
  9. Canepa M, Fonseca C, Chioncel O, Laroche C, Crespo-Leiro MG, Coats AJS, *et al.* Performance of prognostic risk scores in chronic heart failure patients enrolled in the European Society of Cardiology Heart Failure Long-Term Registry. *JACC Heart Fail* 2018;**6**:452-462. doi:10.1016/j.jchf.2018.02.001
  10. Levy WC, Mozaffarian D, Linker DT, Sutradhar SC, Anker SD, Cropp AB, *et al.* The Seattle heart failure model: Prediction of survival in heart failure. *Circulation* 2006;**113**:1424-1433. doi:10.1161/CIRCULATIONAHA.105.584102
  11. O'Connor CM, Whellan DJ, Wojdyla D, Leifer E, Clare RM, Ellis SJ, *et al.* Factors related to morbidity and mortality in patients with chronic heart failure with systolic dysfunction: The HF-action predictive risk score model. *Circ Heart Fail* 2012;**5**:63-71. doi:10.1161/CIRCHEARTFAILURE.111.963462
  12. Pocock SJ, Wang D, Pfeffer MA, Yusuf S, McMurray JJ, Swedberg KB, *et al.* Predictors of mortality and morbidity in patients with chronic heart failure. *Eur Heart J* 2006;**27**:65-75. doi:10.1093/eurheartj/ehi555
  13. Carlsson G. *Bulletin (new series) of the American Mathematical Society* 2009;**46**:255-308. doi:10.1090/S0273-0979-09-01249-X
  14. Dagliati A, Geifman N, Peek N, Holmes JH, Sacchi L, Bellazzi R, *et al.* Using topological data analysis and pseudo time series to infer temporal phenotypes from electronic health records. *Artif Intell Med* 2020;**108**:101930. doi:10.1016/j.artmed.2020.101930
  15. Li L, Cheng WY, Glicksberg BS, Gottesman O, Tamler R, Chen R, *et al.* Identification of type 2 diabetes subgroups through topological analysis of patient similarity. *Sci Transl Med* 2015;**7**:311ra174. doi:10.1126/scitranslmed.aaa9364
  16. Casaclang-Verzosa G, Shrestha S, Khalil MJ, Cho JS, Tokodi M, Balla S, *et al.* Network tomography for understanding phenotypic presentations in aortic stenosis. *JACC Cardiovasc Imaging* 2019;**12**:236-248. doi:10.1016/j.jcmg.2018.11.025
  17. Myasoedova VA, Chiesa M, Cosentino N, Bonomi A, Ludergrani M, Bozzi M, *et al.* Non-stenotic fibro-calcific aortic valve as a predictor of myocardial infarction recurrence. *Eur J Prev Cardiol* 2024; doi:10.1093/eurjpc/zwae062
  18. Kardos A. Association between aortic valve sclerosis and re-infarction after first myocardial infarction points towards a common pathway. Results of an observational study using topological data analysis. *Eur J Prev Cardiol* 2024; doi:10.1093/eurjpc/zwae097
  19. Agostoni P, Bianchi M, Moraschi A, Palermo P, Cattadori G, La Gioia R, *et al.* Work-rate affects cardiopulmonary exercise test results in heart failure. *Eur J Heart Fail* 2005;**7**:498-504. doi:10.1016/j.ejheart.2004.06.007
  20. Agostoni P, Dumitrescu D. How to perform and report a cardiopulmonary exercise test in patients with chronic heart failure. *Int J Cardiol* 2019;**288**:107-113. doi:10.1016/j.ijcard.2019.04.053
  21. Hansen JE, Sue DY, Wasserman K. Predicted values for clinical exercise testing. *Am Rev Respir Dis* 1984;**129**:S49-S55. doi:10.1164/arrd.1984.129.2P2.S49
  22. Shannon P, Markiel A, Ozier O, Baliga NS, Wang JT, Ramage D, *et al.* Cytoscape: A software environment for integrated models of biomolecular interaction networks. *Genome Res* 2003;**13**:2498-2504. doi:10.1101/gr.1239303
  23. Girvan M, Newman ME. Community structure in social and biological networks. *Proc Natl Acad Sci U S A* 2002;**99**:7821-7826. doi:10.1073/pnas.122653799
  24. Trapnell C, Cacchiarelli D, Grimsby J, Pokharel P, Li S, Morse M, *et al.* The dynamics and regulators of cell fate decisions are revealed by pseudotemporal ordering of single cells. *Nat Biotechnol* 2014;**32**:381-386. doi:10.1038/nbt.2859
  25. McInnes L, Healy J, Melville J. Umap: Uniform manifold approximation and projection for dimension reduction. 2018; doi:10.48550/arXiv.1802.03426
  26. Street K, Risso D, Fletcher RB, Das D, Ngai J, Yosef N, *et al.* Slingshot: Cell lineage and pseudotime inference for single-cell transcriptomics. *BMC Genomics* 2018;**19**:477. doi:10.1186/s12864-018-4772-0
  27. Therneau TM, Grambsch PM. *Modeling survival data: Extending the Cox model.* New York: Springer-Verlag; 2000. doi:10.1007/978-1-4757-3294-8
  28. Adamopoulos S, Miliopoulos D, Piotrowicz E, Snoek JA, Panagopoulou N, Nanas S, *et al.* International validation of metabolic exercise test data combined with cardiac and kidney indexes (MECKI) score in heart failure. *Eur J Prev Cardiol* 2023;**30**:1371-1379. doi:10.1093/eurjpc/zwad191
  29. Breiman L. Random forests. *Machine Learning* 2001;**45**:5-32. doi:10.1023/A:1010933404324
  30. Doust J, Lehman R, Glasziou P. The role of BNP testing in heart failure. *Am Fam Physician* 2006;**74**:1893-1898.
  31. Gheorghiadu M, De Luca L, Fonarow GC, Filippatos G, Metra M, Francis GS. Pathophysiological targets in the early phase of acute heart failure syndromes. *Am J Cardiol* 2005;**96**:11G-17G. doi:10.1016/j.amjcard.2005.07.016
  32. Weldy CS, Ashley EA. Towards precision medicine in heart failure. *Nat Rev Cardiol* 2021;**18**:745-762. doi:10.1038/s41569-021-00566-9
  33. Krittanawong C, Zhang H, Wang Z, Aydar M, Kitai T. Artificial intelligence in precision cardiovascular medicine. *J Am Coll Cardiol* 2017;**69**:2657-2664. doi:10.1016/j.jacc.2017.03.571
  34. Sengupta PP, Shrestha S, Kagiya N, Hamirani Y, Kulkarni H, Yanamala N, *et al.* A machine-learning framework to identify distinct phenotypes of aortic stenosis severity. *JACC Cardiovasc Imaging* 2021;**14**:1707-1720. doi:10.1016/j.jcmg.2021.03.020
  35. Hwang D, Kim HJ, Lee SP, Lim S, Koo BK, Kim YJ, *et al.* Topological data analysis of coronary plaques demonstrates the natural history of coronary atherosclerosis. *JACC Cardiovasc Imaging* 2021;**14**:1410-1421. doi:10.1016/j.jcmg.2020.11.009

## Appendix A

Other participants to the MECKI score group to be acknowledged:

- Centro Cardiologico Monzino, IRCCS, Milan, Italy: Stefania Farina, Beatrice Pezzuto, Pietro Palermo, Mauro Contini, Paola Gugliandolo, Irene Mattavelli, Michele Della Rocca, Giulia Grilli
- Department of Clinical and Molecular Medicine, Azienda Ospedaliera Sant'Andrea, 'Sapienza' Università degli Studi di Roma, Roma, Italy: Giovanna Gallo; Emiliano Fiori
- Dipartimento di Scienze Cardiovascolari, Respiratorie, Nefrologiche, Anestesiologiche e Geriatriche, 'Sapienza', Rome University, Rome, Italy: Federica Moscucci
- UOC Cardiologia, G da Saliceto Hospital, Piacenza, Italy: Geza Halasz, Bruno Capelli
- Cardiologia SUN, Ospedale Monaldi (Azienda dei Colli), Seconda Università di Napoli, Napoli: Giuseppe Pacileo, Fabio Valente, Rossella Vastarella, Rita Gravino
- Cardiovascular Department, Ospedali Riuniti and University of Trieste, Trieste, Italy: Maddalena Rossi, Cosimo Carriere, Nikita Baracchini, Teresa Capovilla, Andrea Di Lenarda
- Istituto Auxologico Italiano, Milan, Italy: Sergio Caravita, Elena Viganò
- Cardiac Rehabilitation Unit, Istituti Clinici Scientifici Maugeri, Scientific Institute of Milan, Milan, Italy: Giovanni Marchese
- Cardiology Division, Santo Spirito Hospital, Roma, Italy: Roberto Ricci, Luca Arcari
- Division of Cardiology, Istituti Clinici Scientifici Maugeri, Institute of Cassano Murge, Bari, Italy: Domenico Scrutinio
- U.O. Cardiologia, S. Chiara Hospital, Trento, Italy: Elisa Battaia, Michele Moretti
- Ospedali Riuniti, Ancona, Italy: Matilda Shkzoza
- Federico II, Naples, Italy: Alberto Marra, Roberta D'Assante, Giulia Crisci
- Ospedale di Foggia, Italy: Armando Ferraretti
- 'S.Maugeri' Foundation, Tradate, Italy: Donatella Bertipaglia;
- Cardiologia Riabilitativa, Ospedali Riuniti, Ancona: Francesca Pietrucci
- Telecardiology Center, National Institute of Cardiology, Warsaw, Poland: Ewa Piotrowicz
- Department of Sports Medicine and Cardiology, Isala, Zwolle, Netherlands: Johan Aernout Snoek
- Department of Cardiology, 'Helena Venizelou' Hospital, Athens, Greece: Niki Panagopoulou
- Department of ICU, 'Evangelismos' Hospital, Athens, Greece: Serafim Nanas,
- Department of Cardiology, University Heart Center Zurich, University of Zurich, Zurich, Switzerland: David Niederseer, Reza Mazaheri
- Department of Cardiology, First Medical Center of PLA General Hospital, Beijing, China: Jing Ma
- Department of Cardiology, Sixth Medical Center of PLA General Hospital, Beijing, China: Yundai Chen
- University Clinical Center of Serbia, Belgrade, Serbia: Dejana Popovic, Petar Seferovic
- Heart Research Institute, Sydney, Australia: Andrew JS Coats
- IRCCS San Raffaele La Pisana, Roma, Italy: Giuseppe M. C. Rosano, Maurizio Volterrani
- Cardiology, Department of Medical and Surgical Specialities, Radiological Sciences, and Public Health, Brescia, Brescia, Italy: Cristina Gussago